

UC Irvine

UC Irvine Previously Published Works

Title

A Fermi Liquid Electronic Structure and the Nature of the Carriers in High- T c Cuprates: A Photoemission Study

Permalink

<https://escholarship.org/uc/item/036480kc>

Journal

Physica Scripta, T31(T31)

ISSN

0031-8949

Authors

Arko, Aj
List, RS
Bartlett, RJ
et al.

Publication Date

1990

DOI

10.1088/0031-8949/1990/t31/037

Copyright Information

This work is made available under the terms of a Creative Commons Attribution License, available at <https://creativecommons.org/licenses/by/4.0/>

Peer reviewed

A Fermi Liquid Electronic Structure and the Nature of the Carriers in High- T_c Cuprates: A Photoemission Study

A. J. Arko, R. S. List, R. J. Bartlett, S.-W. Cheong, Z. Fisk and J. D. Thompson

Los Alamos National Laboratory, P-10 Group, Los Alamos, NM 87545, U.S.A.

C. G. Olson, A.-B. Yang, R. Liu and C. Gu

Ames National Laboratory – USDOE, Iowa State University, Ames, Iowa 50011, U.S.A.

B. W. Veal, J. Z. Liu, A. P. Paulikas, K. Vandervoort, H. Claus and J. C. Campuzano

Materials Science Division, Argonne National Laboratory, Argonne, IL 60439, U.S.A.

and

J. E. Schriber and N. D. Shinn

Sandia National Laboratories, Albuquerque, NM 87185, U.S.A.

Received July 20, 1989

Abstract

We have performed angle-integrated and angle-resolved photoemission measurements at 20 K on well-characterized single crystals of high T_c cuprates (both 1:2:3-type and 2:2:1:2-type) cleaved *in situ*, and find a relatively large, resolution limited Fermi edge which shows large amplitude variations with photon energy, indicative of band structure final state effects. The lineshape of the spectra of the 1:2:3 materials as a function of photon energy are well reproduced by band structure predictions, indicating a correct mix of $2p$ and $3d$ orbitals in the calculations, while the energy positions of the peaks agree with calculated bands to within ≈ 0.5 eV. This may yet prove to reflect the effects of Coulomb correlation. We nevertheless conclude that a Fermi liquid approach to conductivity is appropriate. Angle-resolved data, while still incomplete, suggest agreement with the Fermi surface predicted by the LDA calculations. A BCS-like energy gap is observed in the 2:2:1:2 materials, whose magnitude is twice the weak coupling BCS value (i.e., $2\Delta \approx 7kT_c$).

1. Introduction

It is widely believed that the electronic structure of the high- T_c superconducting (HTSC) cuprates consists of impurity bands induced by the doping of holes into the CuO_2 planes. Many theoretical models [1] assume that the underlying electronic structure is not substantially altered by the doping so that the electronic structure of the HTSCs is similar to the non-superconducting (or insulating) parent compounds. Since band calculations [2–7], using the local density approximation (LDA), have been singularly unsuccessful in predicting the magnetic and insulating properties of the parent oxides, it is a natural extension to assume that such calculations are inapplicable to HTSCs. The general approaches (aside from band structure) that have been taken include the Anderson model [8, 9], some variant of the Hubbard model [10–13] and the resonating valence bond model [14]. To the best of our understanding the last approach results in charge carriers which do not strictly obey Fermi–Dirac statistics so that the system is not described as a Fermi liquid with a well-defined Fermi surface.

Early photoemission measurements, both angle-integrated [15–19] and angle-resolved [20, 21] using single crystals, in

fact seemed to support the more exotic approaches. While a very small, well-defined Fermi edge was occasionally observed [16] in La–Sr–Cu–O systems, it was never seen in the 1:2:3 type materials [22], thus reinforcing the concept of a vanishingly small density of states (DOS) at E_F and no conventional Fermi function cutoff of normal metals.

The discovery of the Bi-based cuprates with their stable Fermi edge at room temperature changed the above situation and initially actually appeared to be inconsistent with the 1:2:3s and 2:1:4s. We showed [23–26], however, that most early photoemission data on these latter types of compounds, if taken at room temperature, probably were not sampling the true bulk electronic structure but rather only a deteriorated surface oxide (an insulator with no DOS at E_F) resulting from surface reconstruction, oxygen loss, or both (the actual mechanism is yet to be determined). If, however, a well-characterized superconducting single crystal of a 1:2:3 material is cleaved at low temperatures ($T < 50$ K) to expose a fresh surface, such a surface reconstruction (and/or oxygen loss) is suppressed and a spectrum representative bulk superconductor is obtained. This is evidenced by the existence of a large, stable Fermi edge and the appearance of a highly structured photoemission spectrum [27] which, as we shall see, is not inconsistent with a band structure DOS. Thus a uniformity regarding the Fermi edge is established among the HTSCs (including the BiO_3 -based compounds) which now makes them strong candidates for Fermi liquids, as will become evident in the text. Indeed it is now possible to observe directly via photoemission the large BCS-like gap [28–30] at temperatures below T_c , and in fact only for those k -values which correspond to the Fermi surface [29, 30].

The weight of evidence is building not only in favour of the Fermi liquid model, but rather also towards an electronic structure in large measure describable by a band structure DOS [27] (at least some form of renormalized bands), and a Fermi surface very similar to predictions. Thus we are apparently not dealing with impurity bands at E_F [31], but rather with bands described by a band calculation. It

remains yet to be determined to what extent the bands are renormalized as a consequence of the strong Coulomb correlation which is evidenced in the form of satellites [16, 32, 33], and whether this correlation plays a significant role in the superconductivity.

In the present manuscript we will review our recent photoemission data which led us to the above conclusions. We will mostly confine ourselves to angle-integrated data since the angle-resolved work is still in progress, although the latter type of data will eventually be much more compelling. We have not studied the parent insulating oxides in any great detail so that we don't know how they differ from the predicted metallic behaviour. This latter study is a necessary step in understanding these materials and is at present underway.

2. Experimental details

A much more detailed set of experimental procedures is published elsewhere [27]. Here we will only concentrate on the essential features.

The angle-integrated photoemission measurements were taken at the Synchrotron Radiation Center in Stoughton, WI, using the Ames-Montana ERG/SEYA beamline, as well as the Minnesota-Argonne-Los Alamos ERG beamline. Overall instrument resolution for the beamline and the double pass CMA analyzer varied from 125 to 200 meV. The chamber pressure was maintained at 5×10^{-11} Torr throughout the measurements. Cooling to 20 K was accomplished via a closed cycle He refrigerator. The angle-resolved data on the 2:2:1:2s reported here was taken with a VSW 50 mm hemispherical analyzer, with a maximum overall resolution (at 2 eV pass energy) of 30 meV. Chamber pressure was likewise maintained at 5×10^{-11} Torr and sample temperature controlled with a He refrigerator.

The thin single crystal plates (typical dimensions 1 mm \times 1 mm \times 0.05 mm) were mounted with epoxy between two Al rods oriented along the c -axis. Electrical contact was made with a thin layer of a suspended graphite solution. One of the Al rods was in contact with the cold finger while prying *in situ* on the free Al rod resulted in a sample cleave in the a - b plane.

Most of the measurements reported here were done with the sample temperature maintained at 20 K since, as will become evident, warming above 50 K resulted in a rapid deterioration of the 1:2:3 surface [23, 24]. On the other hand, the sample surface remained stable for up to 2 days if maintained at 20 K. A similar instability was not observed for the 2:2:1:2s.

3. Results and discussion

3.1. Clean vs. deteriorated surface of Y-1:2:3

In Fig. 1 we show 3 spectra from a Y:1:2:3- $O_{6.9}$ crystal cleaved at 20 K and measured first at 20 K, then at 300 K and again at 20 K. A measurement at 20 K immediately after a fresh cleave (20_i in Fig. 1) exhibits a large, resolution-limited Fermi edge, and a substantial spectral weight in the -1 eV to -2 eV range. It does not, however, show the much discussed [34, 35] feature at -9 eV. If the sample is maintained at 20 K the spectrum 20_i can be reproduced indefinitely.

Warming to 300 K, however, immediately results in dramatic changes. Even before the -9 eV features develops significant intensity, the spectrum loses *all* the intensity at E_F ,

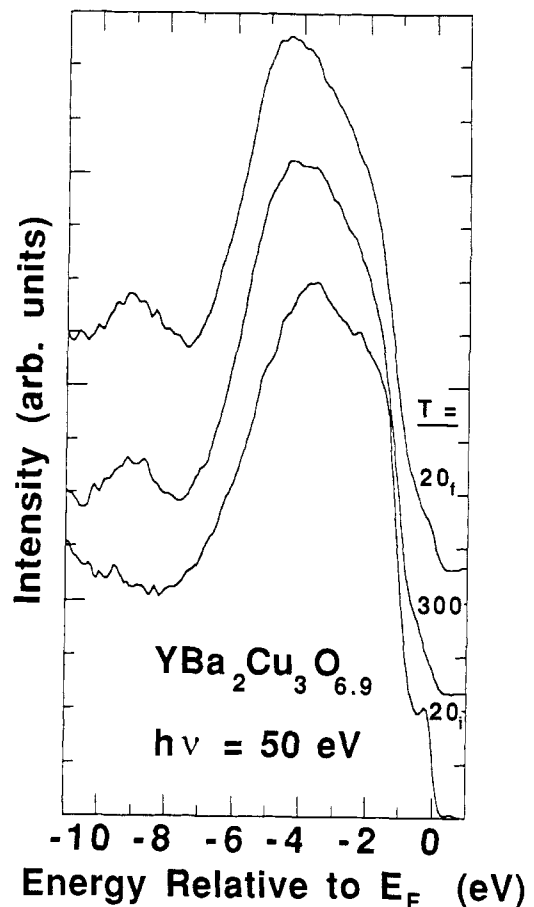


Fig. 1. Valence band spectra for a crystal of $YBa_2Cu_3O_{6.9}$ in the a - b plane. Sample was cleaved at 20 K. Lowest curve, 20_i, was taken immediately after the cleave, the middle curve was taken within 10 min. of warming to 300 K, while the top curve was again taken at 20 K upon re-cooling. Note the irreversibility of the various spectral changes (see Text).

followed by a substantial loss of intensity in the -1 to -2 eV range, a valence band maximum shift from -3.5 eV to -4.5 eV, and additional intensity loss near -6 eV. Cooling the sample back to 20 K (spectrum 20_f in Fig. 1) shows that the changes are irreversible, although some apparent recovery is seen near E_F . This recovery is not understood at present but may be related to a phase transition.

It is instructive to follow the behaviour of the O-1s core level as the surface deteriorates. In Fig. 2 we show three spectra of this core level. Spectrum (a) is for $Bi_2Sr_2CaCu_2O_8$ after a fresh cleave at 20 K, spectrum (b) is for Y:1:2:3- $O_{6.9}$ (same sample as in Fig. 1) likewise after a fresh cleave, while spectrum (c) is for the same sample of Y:1:2:3 but now at 300 K. Note that a single O-1s core level is found at -528 eV in both materials after a fresh cleave. As the surface of the 1:2:3 material deteriorates, a second O-1s peak at -531 eV grows along with the -9 eV peak. Some researchers have assigned [36, 37] the -531 eV peak to the O^{1-} valence state (vs. the O^{2-} for the -528 eV peak). However, we can see that it is not intrinsic to the $O_{6.9}$ material.

The question arises whether the deterioration is due to oxygen loss resulting in an oxygen deficient Y:1:2:3 surface, or to a chemical change [38] resulting in a totally different composition at the surface. We can get some insight by studying well-characterized oxygen-deficient crystals cleaved and measured under identical conditions as the $O_{6.9}$ sample. The spectra for several $YBa_2Cu_3O_x$ materials are shown in

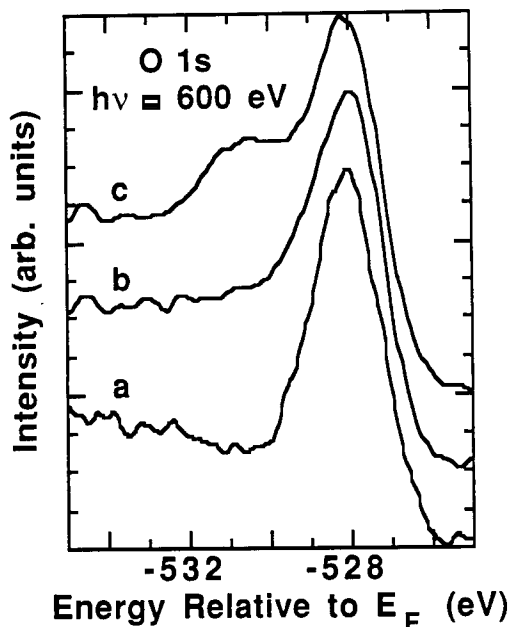


Fig. 2. O-1s core level spectra showing the single line nature of the clean spectra; (a) $\text{Bi}_2\text{Sr}_2\text{CaCu}_2\text{O}_8$ at 20 K after a fresh cleave; (b) $\text{YBa}_2\text{Cu}_3\text{O}_{6.9}$ at 20 K after a fresh cleave; (c) $\text{YBa}_2\text{Cu}_3\text{O}_{6.9}$ after $\approx 1/2$ hr at 300 K. Note the buildup of a feature at -531 eV as the surface deteriorates.

Fig. 3 at $h\nu = 50$ eV. We can see that while the DOS at E_F decreases monotonically with x , there is no indication of the -9 eV peak in any spectrum, and the valence band maximum remains at -3.5 eV for all x . There is, however, a significant

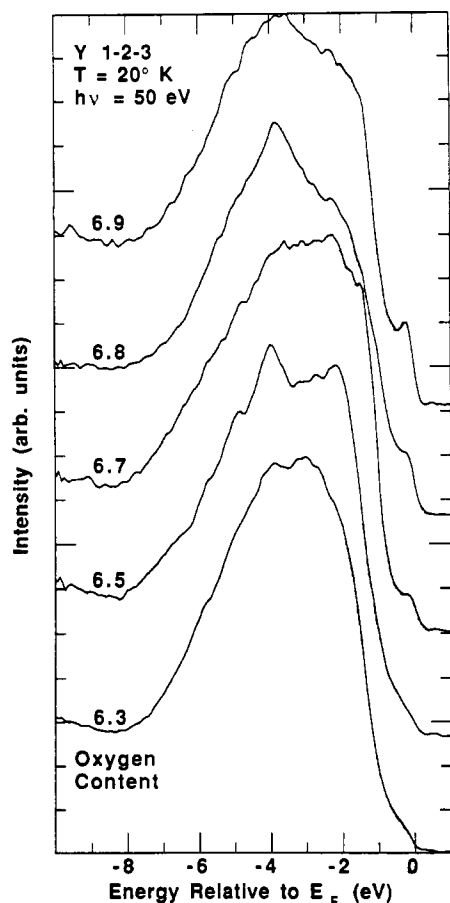


Fig. 3. Valence band spectra for $\text{YBa}_2\text{Cu}_3\text{O}_x$ at $h\nu = 50$ eV for values of x between 6.25 and 6.9, taken on crystals cleaved and measured at 20 K. The -9 eV satellite is absent for all values of x . Note the decrease in $N(E_F)$ as x decreases. Note also that the valence band maximum is at ≈ 3.5 eV for all x .

narrowing of the valence band width for $x = 6.25$, with significant accompanying intensity losses at -1.5 eV.

We conclude from Fig. 3 that while decreasing the oxygen content does indeed cause some changes throughout the valence bands, a spectrum taken at room temperature on a deteriorated surface is totally unrelated to that of a 1:2:3 material. Perhaps some oxygen loss is occurring. However, a more significant factor for UV photoemission measurements with their small escape depths is a composition change [38] on the surface which yields the -9 eV feature in the valence bands, as well as the -531 eV peaks in the O-1s spectrum. Thus attempts to correlate these features with valence fluctuations or other phenomena intrinsic to the 1:2:3 materials, are in error.

3.2. Valence bands of Y:1:2:3; comparison to band calculations

Having established the instability of the 1:2:3 surface at

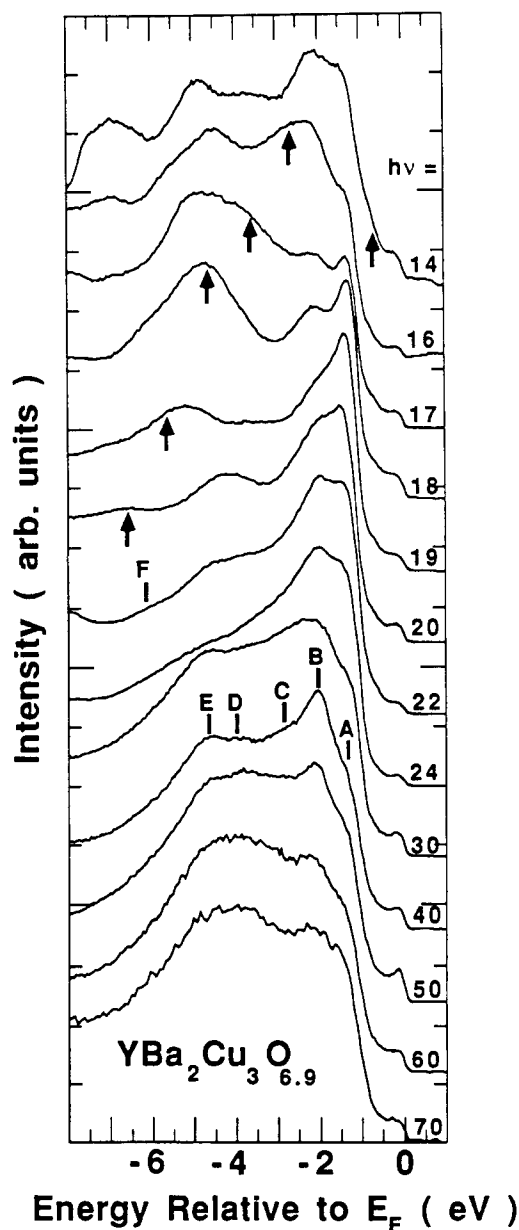


Fig. 4. Angle-integrated valence band spectra for $\text{YBa}_2\text{Cu}_3\text{O}_{6.9}$ for values of $h\nu$ ranging from 14 to 70 eV. The apparent dispersion below $h\nu \approx 20$ eV is due to van Hove singularities in the empty state (see Text). The amplitude modulation of the Fermi edge with $h\nu$ is due to the same phenomenon. Peaks A through F can be identified with the DOS.

elevated temperatures, it is clear that meaningful data can only be obtained on a freshly-cleaved single crystal surface at $T < 50$ K. The bulk of the remaining data was taken under such conditions.

In Fig. 4 we display a series of angle integrated spectra from a sample of $\text{YBa}_2\text{Cu}_3\text{O}_{6.9}$ taken at various photon energies ranging from 14 eV to 70 eV. We point out that these spectra are from a sample different from that of Fig. 1. This caution is necessary since it is evident that at $h\nu = 50$ eV the spectra from the two samples are not identical. The differences are due to residual angle resolved effects stemming from the fact that we are using single crystals and a CMA analyzer which admits only a limited number of electron trajectories. Hence we do not have a true angle integrated spectrum. These phenomena would however tend to affect amplitudes more than peak positions in these very complex materials so that it does not alter our conclusions. We wish to call attention to the following observations:

(a) At low $h\nu$ (< 20 eV) we observe a number of peaks in the secondary electron spectrum due to van Hove singularities in the empty bands [39]. These peaks shift linearly with photon energy to apparent higher binding energies as $h\nu$ increases. There are several sets of such peaks. In Fig. 4 we have marked by arrows one set which leads to the enhancement at E_F for $h\nu = 14$ eV. The very large enhancement of the -1 eV feature at $h\nu = 19$ eV suggests another such set of final state peaks which would coincide with E_F at $h\nu = 18$ eV. These peaks are not representative of the filled states except insofar as they will enhance a valence band feature whenever direct transitions are possible into these van Hove singularities from the filled states. Thus most of the apparent dispersion for $h\nu < 20$ eV is due to these final state effects.

(b) In addition to the peak at E_F , we can identify peaks A through F as being part of the DOS structure.

(c) The Fermi edge amplitude is strongly modulated by the same band structure effects as in (a), but remains strong for all $h\nu$, thus indicating at least a partial d -wave function character (see below).

When one compares the peaks in the spectra to a calculated [2-7] DOS (Fig. 5) it is possible to get a one-to-one correspondence between the calculated and experimentally observed peaks, provided that the calculated Fermi energy is shifted up (to lower binding energies) by 0.5 eV. We show in Fig. 5 a DOS from Ref. [6], although most calculated band

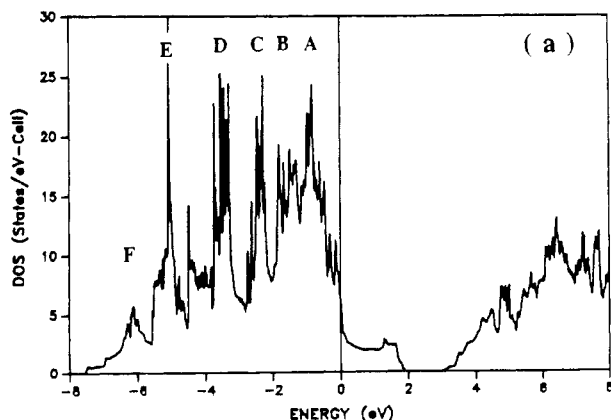


Fig. 5. Density of states taken from ref. [6]. The peaks labeled A through F have a one-to-one correspondence with peaks A through F in Fig. 4 if the calculated Fermi energy is shifted by 0.5 eV to lower binding energy.

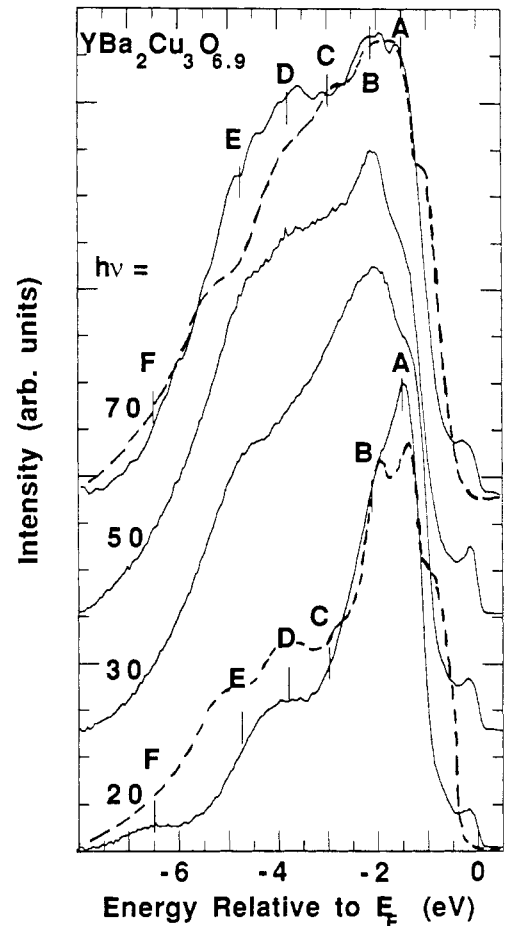


Fig. 6. Comparison of calculated and measured photoelectron spectra. Solid lines are spectra taken from Fig. 4 but with the secondary background subtracted. Dashed lines are calculated spectra from Ref. [41]. Good correspondence is again obtained if we employ the 0.5 eV shift.

structures are similar. Peaks A and B are primarily due to p -like bands while the bulk of the $\text{Cu-}3d$ density is centered around peaks C and D. The weak peak F is due to the bottom of the oxygen- p bonding bands.

The actual character of peaks A through F can be more easily discerned from the lineshapes of the spectra as a function of photon energy. Because of the very different cross sections [40] for p vs. d transitions, the spectral weight changes as $h\nu$ increases. Redinger *et al.* [41] have calculated the expected photoemission spectra as a function of $h\nu$ based on their DOS. We compare several of the spectra of Fig. 4 to these predicted spectra in Fig. 6. The solid curves are spectra from Fig. 4 with backgrounds subtracted, while the dashed curves are from Ref. [41]. The spectra were aligned on the p -like peak A. Except for the 0.5 eV shift we see that the spectral shape follows the correct energy dependence, thus indicating a correct orbital character mix in the DOS. On this gross scale, then, band calculations correctly capture the essential feature of the experimental DOS. The main disagreement is the 0.5 eV shift and the very large predicted Fermi edge (large $N(E_F)$) vs. a much more modest one observed experimentally.

A very recent publication [42] has focused on the problem of Coulomb correlation and how it should effect the band structure as obtained from an LDA calculation. Indeed, they find that for a value of $U \sim 4.0$ eV, the Fermi energy would shift by ≈ 0.5 eV with a corresponding dramatic drop in

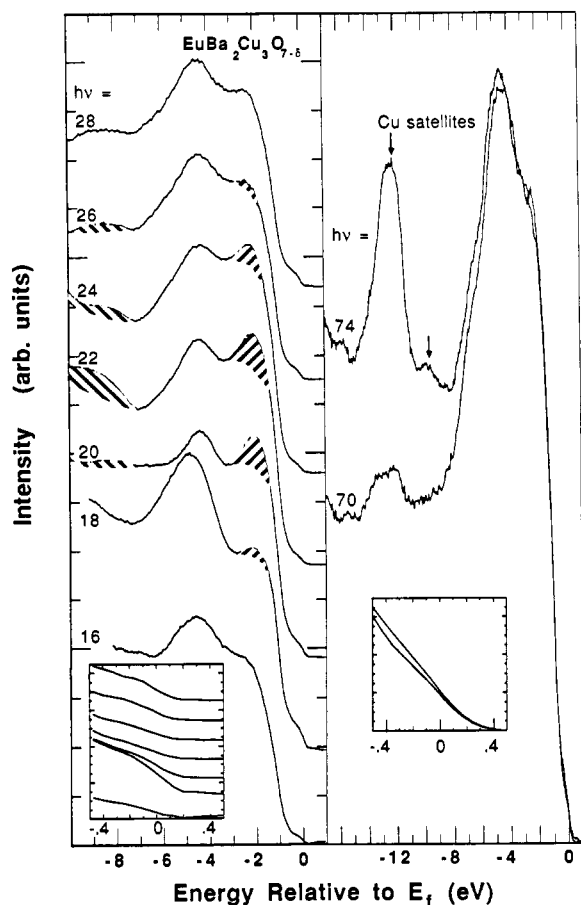


Fig. 7. Spectra taken on a slightly deteriorated sample of $\text{EuBa}_2\text{Cu}_3\text{O}_{7.5}$ in order to see the resonance of the -9 eV contamination peak. Left panel: O-2s absorption edge. An incidental Eu-4f resonance at -5 eV for a photon energy of $h\nu = 18\text{ eV}$ is also observed. Right panel: Cu-3p absorption edge. A large resonant enhancement is observed in the -10 eV and -12 eV Cu-related satellites, while almost no enhancement is seen in the valence bands.

$N(E_F)$, just as observed. This fact, combined with the obvious satellite structure associated with Cu features, would seem to support a band structure at least partially renormalized by Coulomb correlation, a situation somewhat reminiscent of heavy Fermions.

3.3. The character of states at E_F

It is quite important to a number of theories [1] to determine the orbital character of the states at E_F . For example, many theories would prefer primarily O-2p character with oxygen hole hopping in the CuO_2 planes as the primary conduction mechanism. While resonant photoemission has been the technique of choice [43] for determining orbital symmetry of photoemission features, a quick glance at Fig. 7 will show that this technique has its shortcomings with respect to HTSC's. Here we show spectra from a slightly deteriorated sample of Eu: 1:2:3 at both the O-2s (left panel) and Cu-3p (right panel) edges. We do this in order to focus on the -9 eV contamination peak, which is known to be of primarily O-2p character, without completely destroying the underlying 1:2:3 DOS. We see that the contamination peak has a maximum amplitude at $h\nu = 22\text{ eV}$, as does the valence band feature at -2 eV below E_F , which we know from Fig. 4 to correspond to peaks A and B in the DOS and which we know is substantially p-like in character. Actually, this intensity

modulation in the -1 to -2 eV range is clearly seen even in Fig. 4 to be centered around $h\nu = 22\text{ eV}$. Moreover, angle-resolved data, which will be discussed in greater detail elsewhere [44], actually show that much of the p-character is concentrated around the Γ -point in the Brillouin zone, and has an intense resonance ($> 200\%$ increase in intensity) at $h\nu = 22\text{ eV}$. Thus we conclude that at least for 1:2:3 type materials, the oxygen resonance is at $h\nu = 22\text{ eV}$ and not at the often quoted [31] 18 eV . The intensity at E_F , on the other hand, has a minimum at $h\nu = 22\text{ eV}$. The Fano resonance, if any, is obscured by the above-mentioned final state effects (van Hove singularities in the empty state) due to band structure. The situation in the 2:2:1:2s is less obvious, but one should nevertheless be on the alert for final state effects.

Similarly at the 3p edge ($h\nu = 74\text{ eV}$) one runs into difficulties. The data in Fig. 7b were normalized to photon flux and show almost no intensity modulation in the valence bands, while the -10 eV and -12 eV Cu satellites (arrows) undergo a very strong resonance. The large apparent increase in the secondary background is the MVV Auger transition accompanying the Fano resonance. The point is that even if there is 3d character at E_F there is no reason to expect its intensity to resonate at $h\nu = 74\text{ eV}$ since the entire valence band fails to resonate.

One can still determine the orbital character by measuring the intensity at E_F as a function of photon energy. In Fig. 8

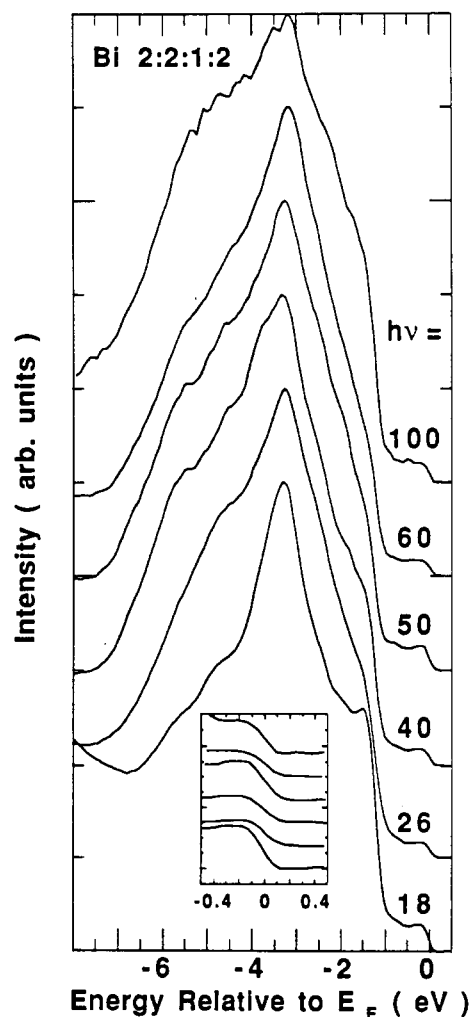


Fig. 8. Valence band spectra for $\text{Bi}_{1.2}\text{Sr}_2\text{CaCu}_2\text{O}_8$ at $T = 20\text{ K}$ for various values of $h\nu$. The intensity of E_F is nearly constant for all spectra except for the final state enhancements at 18 eV and 50 eV .

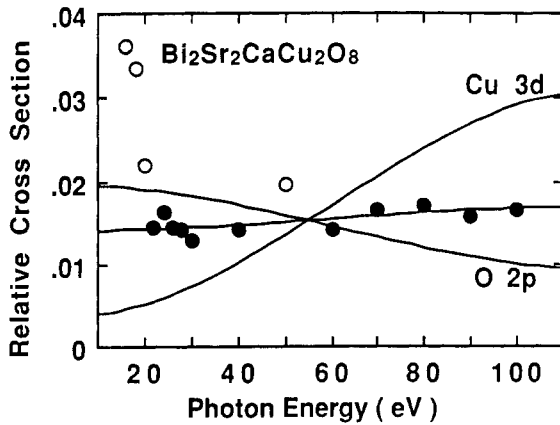


Fig. 9. Plot of the photoemission cross-section at E_F for $\text{Bi}_2\text{Sr}_2\text{CaCu}_2\text{O}_8$ for properly normalized spectra (see Text) for values of $h\nu$ from 18 eV to 100 eV. Open circles represent final state enhancements and are not modeled in the fit. The pure Cu-3d and O-2p cross-sections shown for comparison are taken from Ref. [40]. The measured cross-section can be obtained from a linear combination of 35% Cu-3d and 65% O-2p.

we display angle integrated spectra of $\text{Bi}_2\text{Sr}_2\text{CaCu}_2\text{O}_8$ for a number of photon energies normalized at the valence band maximum. While this is an incorrect normalization procedure one nevertheless sees that the intensity of the peak near E_F (actually at -0.2 eV) remains strong to high photon energies, and shows final state enhancements at 18 eV and 50 eV.

A more correct normalization takes into account the number of p - and d -electrons (we ignore all the rest due to weak cross-sections [40]) and equates the total integrated intensity of the spectrum at each photon energy to the total integrated intensity expected at that energy from the atomic calculations of Yeh and Lindau [40]. The resulting intensity at -0.2 eV is plotted as a function of $h\nu$ in Fig. 9. Here the open circles correspond to values of $h\nu$ where final state enhancements occur and hence are not included in the calculations. The solid lines are intensity variations expected if the features are either entirely d -like or p -like. Clearly the measured intensity follows neither curve. Instead we try to approximate it by taking linear combinations of the two cross-sections and find a best fit with $\approx 35\%$ Cu-3d and 65% O-2p character. Similar analyses for the 1 : 2 : 3 material yield about a 20–80 mix of Cu and O at E_F .

It is difficult to put error bars on these numbers since, as we have seen, the intensity, especially at E_F , is a strong function of the sample surface condition, as well as sample orientation (recall that our measurements are not truly angle integrated). Suffice it to say that there are strong contributions from both Cu and O in the conduction band. This, then, also argues in favour of a strongly-hybridized band-like model.

3.4. Angle-dispersive bands and the BCS-like energy gap

Angle resolved photoemission may in the end prove to be the most significant measurement with which to probe the electronic structure of HTSCs, and a substantial amount of angle-resolved data already exists in literature [31, 45, 46]. We would caution the reader, however, to be cognizant of the very serious sample-dependence encountered. We would automatically discard, for example, any room temperature data on 1 : 2 : 3 samples even though a weak Fermi edge may be evident (refer to Fig. 1). Likewise we are wary of data which features the -9 eV satellite. In the case of the 2 : 2 : 1 : 2

materials we would point out that the Fermi edge in our samples (Fig. 8) is much stronger than in most other published data [31, 46], presumably reflecting sample perfection. On top of all this are the very strong final state modulation effects which greatly increase the parameter space in which to map out the bands. In other words, the absence of a peak in the spectrum does not automatically translate into the absence of a band. It may be missing because of a weak matrix element (i.e., no final state exists for direct transitions at that $h\nu$).

Most published angle-resolved data [31] were taken at $h\nu = 18$ eV, because it is generally believed that a resonant enhancement occurs there. We, however, would not rule out the possibility that for $h\nu = 18$ eV one merely enhances one part of the Brillouin zone due to final state effects, so that a failure to work at other values of $h\nu$ precludes a proper sampling of other parts of the zone. In addition, strong polarization effects have been observed suggesting that one should not rely too heavily on symmetry.

Our own angle resolved work is still in progress, with indications that this will be a long project, indeed. We are not prepared to make definitive statements at this time. However, preliminary indications are that the Fermi surfaces predicted both for the 1 : 2 : 3-type and the 2 : 2 : 1 : 2-type materials will be borne out experimentally. The bands themselves, however, are difficult to follow below ≈ 300 meV in $\text{Bi}_2\text{Sr}_2\text{CaCu}_2\text{O}_8$ so

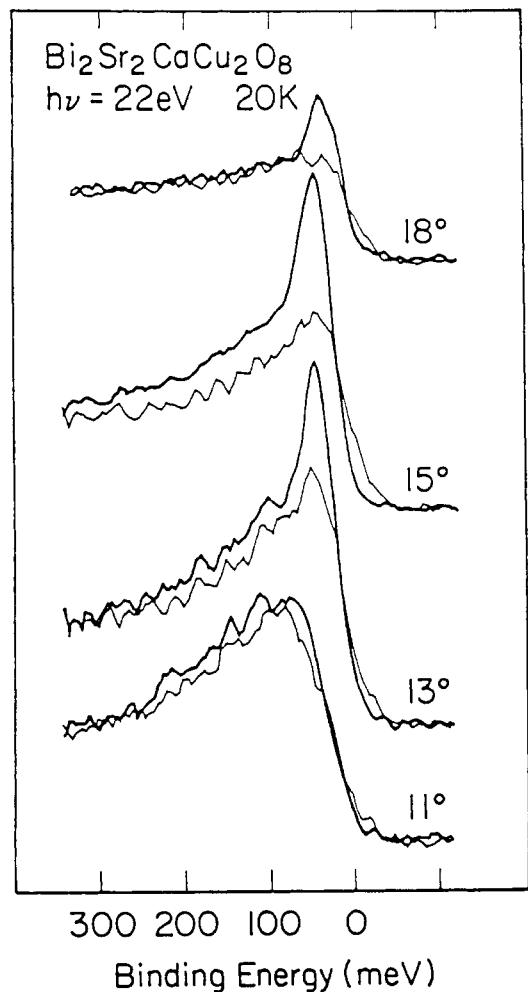


Fig. 10. Angle-resolved valence band spectra within 300 meV of E_F for $\text{Bi}_2\text{Sr}_2\text{CaCu}_2\text{O}_8$ at $h\nu = 22$ eV. Thin lines are data taken at 90 K (above $T_c = 85$ K), and thick lines are data taken at 20 K. The indicated angles, Θ , are with respect to the c -axis and approximately along the Γ -M direction. Note the pile-up of BCS states for the $T = 20$ K data for $\Theta \geq 13^\circ$; i.e., for occupied bands within Δ of E_F .

that we cannot make definitive statements about bandwidths. We do, however, find less disagreement in general with calculated bands than others have observed.

In this manuscript we will confine ourselves to the more definitive aspects of the data. In Fig. 10 we show a series of spectra taken on $\text{Bi}_2\text{Sr}_2\text{CaCu}_2\text{O}_8$ at the indicated angles with respect to the c -axis at $h\nu = 22$ eV. For this set of data, k is approximately along the Γ -M direction. Two sets of data are shown for each angle setting of the analyzer (2° acceptance angle); thin lines correspond to spectra obtained at $T = 90$ K (i.e., at $T > T_c = 85$ K), while the thicker lines correspond to data taken at $T = 20$ K $\ll T_c$. It will be noticed that for an analyzer setting of $\Theta = 11^\circ$ the peak maximum in the spectrum is at -100 meV, well below E_F , and easily resolvable with our overall instrument resolution of 30 meV. In short, the band is still below the Fermi energy and not involved in conduction. At $\Theta = 13^\circ$, however, the band disperses much closer to E_F and the 90 K spectra are vastly different from the 20 K spectra. This is the effect of the BCS-like gap, Δ , at E_F and the associated pile-up of states just below Δ .

Before discussing the effect of the gap in more detail, let us first concentrate on the 90 K spectra. For $\Theta = 18^\circ$ there is a clear indication of the band crossing E_F as evidenced by the dramatic drop in intensity. Because the above data were not taken precisely along a symmetry axis, there is no direct band calculation for comparison. Nevertheless the crossing is approximately in the location where one would expect the M-centered Fermi surface. Data presently being analyzed on better oriented samples appear to indicate nearly exact agreement with the predicted Fermi surface [47].

Because of our 2° acceptance cone of photoemitted electrons, each spectrum in Fig. 10 is simultaneously sampling approximately 10% of the Γ -M momenta ($\approx 0.075 \text{ \AA}^{-1}$). However, for $\Theta = 18^\circ$, most of the band being sampled has dispersed above E_F and we can get a much more accurate measure of the sharpness of the Fermi edge and how it compares to what one expects from a conventional metal. Using the usual 10% to 90% of peak height to determine the width of the Fermi edge, we obtain a value of ≈ 45 meV. Using the same criteria for the Fermi function broadening, the Fermi edge at $T = 90$ K is expected to be broadened by ≈ 35 meV (note that $kT \approx 8$ meV at this temperature) while instrument broadening is ≈ 30 meV. The r.m.s value of these two broadenings is 46 meV which is almost exactly our observed value. Thus we have an electronic structure which obeys Fermi-Dirac statistics—in short, a Fermi liquid!

Returning to the 20 K spectra we note the pile-up of states which results in the sharp peaks (FWHM = 30 meV or, the instrument resolution) just below the gap, Δ . To determine Δ we modeled [30] the $\Theta = 18^\circ$ spectrum with a Lorentzian and a linear term (because of the finite angular acceptance of the analyzer this was again deemed the least complicated spectrum). The width of the 90 K Lorentzian was determined empirically (presumably a function of lifetime broadening and dispersion of initial and final state bands). This was then convolved with a 90 K Fermi function and instrument broadening to obtain a best fit. Finally the “best fit” Lorentzian was convolved with a BCS density of state functions [48] and a 20 K Fermi function. In this way a best fit to the data at 20 K was obtained for $2\Delta = 7kT_c$. This is similar to values previously reported [28, 29], although our data are much more free of complications resulting from angle integration.

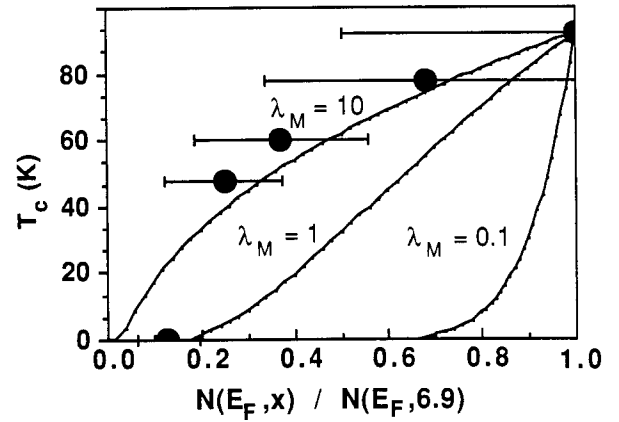


Fig. 11. Plot of the intensity at E_F from Fig. 3 (data points) as a function of T_c . Note the approximate $[N(E_F)]^{1/2}$ variation. Solid lines are plots of the equation $T_c = A(e^{-2\lambda_{\max}/\lambda} - 1)$ for the indicated values of λ_{\max} . The prefactor A is adjusted so that $T_c = 92$ K for each λ_{\max} .

A cursory measurement of the amplitude of the BCS density of states (i.e., a simple scaling of excess peak height vs. temperature) indicates that the pile-up of states with temperature roughly follows a BCS function.

The very large gap (twice the BCS weak coupling value) may be indicative of strong coupling effects in accordance with the results of Kresin [49], who has shown that the limiting value for extremely strong coupling is $8kT_c$. Indeed we have additional evidence [50] from the variation of $N(E_F)$ with T_c that strong coupling effects may be indicated. In Fig. 3 we see that $N(E_F)$ (actually we use the maximum value of the spectral density just below E_F) drops very rapidly with T_c . Kresin in fact has shown from the generalized Eliashberg equations that in the generalized case for any value of the coupling constant, λ ,

$$T_c = 0.5 \langle \omega^2 \rangle^{1/2} (e^{2/\lambda} - 1)^{-1/2}$$

where the prefactor $A = 0.5 \langle \omega^2 \rangle^{1/2}$, is related to the Debye temperature and is allowed to vary to obtain the necessary T_c . If we make the assumption that, as in the BCS formulation, $\lambda = N(E_F)V$, where V is a constant interaction strength, then λ is proportional to $N(E_F)$. In Fig. 11 we plot a series of curves for the function

$$T_c = A(e^{2\lambda_{\max}/\lambda} - 1)^{-1/2},$$

where A and λ_{\max} for each curve are adjusted so that $T_c = 92$ K at $\lambda = \lambda_{\max}$. In the limiting case of large λ_{\max} we have $T_c = 92(\lambda/\lambda_{\max})^{1/2}$ or, equivalently,

$$T_c = 92[N(E_F)/N(E_F)_{\max}]^{1/2}.$$

Here $N(E_F)_{\max}$ is the value of $N(E_F)$ for the $T_c = 92$ K material. We can see from the figure that, while the error bars are large, T_c varies approximately as $[N(E_F)]^{1/2}$, or the strong coupling limit.

4. Conclusions

We believe that there is ample indication that band structure calculations have captured the essential features of the DOS in HTSC materials. While some renormalization of the bands due to the electron–electron correlation effects may still prove necessary, the indications are that we are dealing with a conventional Fermi liquid whose Fermi surface is adequately

described by LDA calculations. A BCS-like energy gap is observed in the 2:2:1:1 materials whose value is about twice the weak-coupling BCS value, but the density of states just below Δ is correctly described by the BCS function. The large gap and the rapid variation of $N(E_F)$ with T_c would seem to support a strong coupling model. Previous inconsistencies in photoemission data are primarily due to the use of sintered materials and measurements at room temperature which yield a surface composition different from the bulk.

Acknowledgements

This work was performed under the auspices of the U.S. Department of Energy. The Ames Lab. acknowledges DOE support under contract #W-7405-ENG82 while Argonne National Lab acknowledges DOE support under contract #W-31-109-ENG-38. The Synchrotron Radiation Center, whose staff we wish to gratefully acknowledge for their assistance, is supported by the NSF under contract #DMR8601349. We wish to acknowledge illuminating discussions with S. Trugman, B. Brandow, F. M. Mueller and R. L. Martin.

References

- For a compilation of the various approaches see, "Theories of High Temperature Superconductivity", (Edited by J. Woods Halley), Addison-Wesley (1988).
- For a complete list of references on various band structure calculations, see the review article by Warren E. Pickett, to be published in *Rev. Mod. Phys.*
- Yu, J., Freeman, A. J. and Xu, J. H., *Phys. Rev. Lett.* **58**, 1035 (1987); Massida, S., Yu, J. and Freeman, A. J., *Phys. Rev.* **B38**, 11352 (1988); Yu, J., Freeman, A. J. and Massida, S., "Novel Superconductivity", (Edited S. A. Wolf and V. Z. Kresin, p. 367. Plenum, New York (1987).
- Mattheiss, L. F. and Hamann, D. R., *Phys. Rev. Lett.* **60**, 2681 (1988).
- Herman, F., Kasowski, R. V. and Hsu, W. Y., *Phys. Rev.* **B38**, 204 (1988); Hus, W. Y. and Kasowski, R. V., "Novel Superconductivity", eds. Wolf, S. A. and Kresin, V. Z., p. 373. Plenum, New York (1987).
- Ching, W. Y., Xu, Yongnian, Zhao, Guang-Lin, Wong, K. W. and Zandiehnam, *Phys. Rev. Lett.* **59**, 1333 (1987).
- Szpunar, B., Smith, V. H. and Smith, R. W., *Physica* **C152**, 91 (1988); Temmerman, W. M., Szotek, Z. and Guo, G. Y., *J. Phys.* **C21**, L867 (1988).
- Fujimori, A. and Minami, F., *Phys. Rev.* **B30**, 957 (1984); Fujimori, A., Saeki, M., Kimizuka, N., Taniguchi, M. and Suga, S., *Phys. Rev.* **B34**, 7318 (1987); Fujimori, A., in "Strong Correlation and Superconductivity", (edited H. Fukuyama, S. Maekawa and A. P. Malozemoff, pp. 1-12 Springer, Berlin (1989).
- van der Laan, G. Westra, C., Haas, C. and Sawatsky, G. A., *Phys. Rev.* **B23**, 4369 (1981); Sawatsky, G. A. and Allen, J. W., *Phys. Rev. Lett.* **53**, 2339 (1985); Zaanen, J., Sawatsky, G. A. and Allen, J. W., *Phys. Rev. Lett.* **55**, 8060 (1986).
- Emery, V., *Phys. Rev. Lett.* **58**, 1196 (1987).
- Zhang, F. C. and Rice, T. M., *Phys. Rev.* **B37**, 3759 (1988).
- Varma, C. M., Schmitt-Rink, S. and Abrahams, E., *Solid State Comm.* **62**, 681 (1987).
- Hirsh, J. E., *Phys. Rev.* **B35**, 8726 (1987).
- Anderson, P. W., *Science* **235**, 1196 (1987); Anderson, P. W., Baskaran, G., Zou, Z. and Hsu, T., *Phys. Rev. Lett.* **58**, 2790 (1987).
- Wendin, G., *J. Phys. (Paris) Colloq.* **48**, C9-483 (1987); Wendin, G., *Physica Scripta*, **T27**, 31 (1989).
- Shen, Z. X., Allen, J. W., Yeh, J. J., Kang, J-S., Ellis, W. P., Spicer, W. E., Lindau, I., Maple, M. B., Dalichauch, Y. D., Torikachhivi, M. S., Sun, J. Z. and Geballe, T. H., *Phys. Rev.* **B36**, 8414 (1987).
- Steiner, P., Albers, J., Kinsinger, V., Sander, I., Siegwort, B., Huffner, S. and Politis, C., *Z. Phys.* **B66**, 275 (1986); Steiner, P., Kinsinger, V., Sander, I., Siegwort, B., Huffner, S., and Politis, C., *Z. Phys.* **B67**, 19 (1987).
- Johnson, P. D., Qui, S. L., Jiang, L., Ruckman, M. W., Strongin, M., Hulbert, S. L., Garrett, R. F., Sinkovic, B., Smith, N. V., Cava, R. J., Lee, C. S., Nichols, D., Koczanowicz, E., Salomon, R. E. and Crow, J. E., *Phys. Rev.* **B35**, 8811 (1987).
- Weaver, J. H., Meyer, H. M., III, Wagener, T. J., Hill, D. M., Gao, Y., Peterson, D., Fisk, Z. and Arko, A. J., *Phys. Rev.* **B38**, 4668 (1988).
- Stoffel, N. G., Chang, Y., Kelly, M. K., Dottl, L., Onellion, M., Morris, P. A. and Bonner, W. A., *Phys. Rev.* **B37**, 7952 (1988); Tang, Ming, Stoffel, N. G., Chen Biao, Qi, La Graffe, D., Morris, P. A., Bonner, W. A., Margaritondo, G. and Onellion, M., *Phys. Rev.* **B38**, 897 (1988).
- Onellion, M., Tang, Ming, Chang, Y., Margaritondo, G., Tarascon, J. M., Morris, P. A., Bonner, W. A. and Stoffel, N. G., *Phys. Rev.* **B38**, 881 (1988).
- A weak irreproducible Fermi edge was reported by Rossi, G., Revcolevschi, A. and Jegoude, J., *Int. J. Mod. Phys.* **B1**, 831 (1987).
- Arko, A. J., List, R. S., Fisk, Z., Cheong, S-W, Thompson, J. D., O'Rourke, J. A., Olson, C. G., Yang, A-B., Pi, T-W., Schirber, J. E. and Shinn, N. D., *J. Mag. Mag. Mater. Lett.* **75**, L1 (1988).
- List, R. S., Arko, A. J., Fisk, Z., Thompson, J. D., Pierce, C. B., Peterson, D. E., Bartlett, R. J., Shinn, N. D., Schirber, J. E., Veal, B. W., Paulikas, A. P. and Campuzano, J. C., *Phys. Rev.* **B38**, (Rapid Comm), 11966 (1988).
- List, R. S., Arko, A. J., Fisk, Z., Cheong, S-W., Conradson, S. D., Thompson, J. D., Pierce, C. B., Peterson, D. E., Bartlett, R. J., O'Rourke, J. A., Shinn, N. D., Schirber, J. E., Olson, C. G., Yang, A-B., Pi, T-W., Veal, B. W., Paulikas, A. P. and Campuzano, J. C., *AIP Conf. Proc.* **182**, 283 (1989).
- List, R. S., Arko, A. J., Fisk, Z., Cheong, S-W., Thompson, J. D., O'Rourke, J. A., Olson, C. G., Yang, A-B., Pi, T-W., Schirber, J. E. and Shinn, N. D., Submitted to *J. Appl. Phys.*
- Arko, A. J., List, R. S., Bartlett, R. J., Cheong, S-W., Fisk, Z., Thompson, J. D., Olson, C. G., Yang, A-B., Liu, R., Gu, C., Veal, B. W., Liu, J. Z., Paulikas, A. P., Vandervoort, K., Claus, H., Campuzano, J. C., Schirber, J. E. and Shinn, N. D., *Phys. Rev.* **B40**, 2286 (1989).
- Imer, J.-M., Patthey, F., Dardel, B., Schneider, W-D., Baer, Y., Petroff, Y. and Zettl, A., *Phys. Rev. Lett.* **62**, 336 (1989).
- Manzke, R., Buslaps, T., Claessen R. and Fink, J., *Europhysics Lett.*, [in Press].
- Olson, C. G., Liu, R., Yang, A-B., Lynch, D. W., Arko, A. J., List, R. S., Veal, B. W., Chang, Y. C., Jiang, P. Z. and Paulikas, A. P., *Science* **245**, 731 (1989).
- Takahashi, T., Matsuyama, H., Katayama-Yoshida, H., Okabe, Y., Hosoya, S., Seki, K., Fujimoto, H., Sato, M. and Inokuchi, H., *Nature* **334**, 691 (1988); Takahashi, T., Matsuyama, H., Katayama-Yoshida, H., Okabe, Y., Hosoya, S., Seki, K., Fujimoto, H., Sato, M. and Inokuchi, H., *Phys. Rev. B* (to be published).
- Sarma, D. D., *Phys. Rev.* **B37**, 7948 (1988).
- Zaanen, J., Sawatsky, G. A. and Allen, J. A., *Phys. Rev. Lett.* **55**, 418 (1985).
- Ford, W. K., Chen, C. T., Anderson, J., Kwo, J., Liou, S. H., Hong, M., Rubenacker, G. V. and Drumheller, J. E., *Phys. Rev.* **B37**, 7924 (1988).
- Stoffel, N. G., Morris, P. A., Bonner, W. A., LaGraffe, D., Tang, Ming, Chang, Y., Margaritondo, G. and Onellion, M., *Phys. Rev.* **B38**, 213 (1988).
- van der Marel, D., van Elp, J., Sawatsky, G. A. and Heitman, D., *Phys. Rev.* **B37**, 5136, (1988).
- Gorieux, T., Krill, G., Maurer, M., Ravet, M. F., Menny, A., Tolentino, H. and Fontaine, A., *Phys. Rev.* **B37**, 7516 (1988).
- Takahashi, T., Maeda, F., Katayama-Yoshida, H., Okabe, Y., Suzuki, T., Fujimori, A., Hosoya, S., Shamoto, S., and Sato, M., *Phys. Rev.* **B37**, 9788 (1988).
- Himpel, F. J., *Applied Optics*, **19**, 3964 (1980).
- Yeh, J. J. and Lindau, I., *Atomic Data and Nuclear Data Tables* **32**, 1 (1985).
- Redinger, J., Freeman, A. J., Yu, J. and Massida, S., *Phys. Lett.* **A124**, 469 (1987).
- Costa-Quintana, J., Lopes-Aguilar, F., Balle, S. and Salvador, R., *Phys. Rev.* **B39**, 9675 (1989).
- Fano, U., *Phys. Rev.* **124**, 1886 (1961).
- Olson, C. G., Liu, R., Lynch, D. W., Veal, B. W., Chang, Y. C., Jiang, P. Z., Liu, J. Z., Paulikas, A. P., Arko, A. J. and List, R. S., in

- Proceedings of the Stanford Conference on High- T_c Superconductivity, Stanford, CA, July 24–28, 1989.
45. Sakisaka, Y., Komeda, T., Maruyama, T., Onchi, M., Kato, H., Aiura, Y., Yanashima, H., Terashima, T., Bando, Y., Iijima, K., Yamamoto, K. and Hirata, K., *Phys. Rev.* **B39**, 2304 (1989); *Phys. Rev.* **B39**, 9080 (1989).
 46. Minami, F., Kimura, T. and Taekawa, S., *Phys. Rev.* **B39**, 4788 (1989).
 47. Massida, S., Yu, J. and Freeman, A. J., **C52**, 251 (1988).
 48. Chang, Y., Tang, Ming, Zanoni, R., Onellion, M., Joynt, R., Huber, D. S., Margaritondo, G., Morris, P. A., Bonner, W. A., Tarascon, J. M. and Stoffel, N. G., *Phys. Rev.* **B39**, 4740 (1989).
 49. Kresin, V. Z., *Phys. Lett.* **A122**, 434 (1987).
 50. Veal, B. W., Olson, C. G., Arko, A. J., List, R. S., Liu, R., Yang, A-B., Gu, C., Bartlett, R. J., Liu, J. Z., Vandervoort, K., Paulikas, A. P. and Campuzano, J. C., *Physica* **C158**, 276 (1989).